USB Proceedings

SDEMPED 2015

10th IEEE International Symposium on Diagnostics for Electric Machines, Power Electronics and Drives

Guarda · Portugal | September 1 - 4, 2015

cise Electromechatronic Systems Research Centre

IEEE Advancing Technology for Humanity

pels

IAS 50 years IEEE Industry Applications Society

ieee

UNIVERSIDADE DA BEIRA INTERIOR Covilhã | Portugal

IPG

GUARDA

USB Proceedings

2015 IEEE 10th International Symposium on Diagnostics for Electrical Machines, Power Electronics and Drives (SDEMPED)

IEEE Catalog Number: CFP15SDE-USB
ISBN: 978-1-4799-7742-0

Bearing damage diagnosis by means of the linear discriminant analysis of stator current feature

Christelle Piantsop Mbo'o and Kay Hameyer

Institute of Electrical Machines (IEM)
www.iem.rwth-aachen.de
RWTH Aachen University
Schinkelstrasse 4, 52062 Aachen, Germany
Email: christelle.piantsop@iem.rwth-aachen.de

***Abstract*—Bearing damage is the most common failure in electrical machines. It can be detected by vibration analysis. However, this diagnosis method is costly or not always accessible due to the location of the equipment and the choice of the implemented sensors. An alternative method is provided with the electrical monitoring using the stator current of the electrical machine. This work aims at developing a diagnostic system based on the current feature generated by a frequency selection in the stator current spectrum. The features are evaluated by means of the linear discriminant analysis (LDA) and the fault diagnosis is performed with the Bayes classifier. The proposed method is evaluated by two types of damages at different load cases. The results show that the damaged bearings can be distinguished from the healthy bearing depending on the considered load cases.**

Keywords*—Bayes classifier, bearing damage, fault diagnosis, linear discriminant analysis, permanent magnet synchronous machine, spectral analysis, stator current.

I. Introduction

Electrical machines consist of several components, which are amongst others: stator, rotor windings, magnets in permanent magnet synchronous machines (PMSMs), shaft or bearings. All these components may be damaged due to abrasion, overloading, unbalanced load or electrical stress because of the control with an inverter. Machine failures can be classified into four groups: bearing damages, damages related to the stator, the rotor and other damages [1]. Bearing damages are the most common fault [2]. The early detection of this failure is an important issue because unexpected breakdown or fatal damage of the entire drive system can be avoided. Moreover, maintenance cost can be reduced and the system reliability is increased by using the condition monitoring. Bearing damage can be detected by vibration analysis [3], [4], [5]. This is a reliable and standardized method for the detection of bearing damage due to fatigue failures, particularly local damages. However, the choice and the positioning of the sensors can be a challenge depending on the location of the equipment. Therefore, the diagnosis using vibration sensors is costly, not always accessible and an online monitoring can not always be guarantee.

An alternative method is given by the electrical monitoring by means of the stator current of the PMSM as well as the induction machine. This method uses the embedded stator current signal of the control unit, so that no additional sensors are required for the detection.

Several paper investigates the detection by means of the stator current [6], [7], [8], [9], [10], [11], [12], [13]. A short overview of the results is presented here to illustrate the objective of this work. For example, Rosero [7] discusses the detection of bearing damage within a PMSM by means of the wavelet as well as the short-time Fourier transform of a simulated non stationary signal of the stator current. The detection using the wavelet transform gives the best results. However the comparison between simulated and experimental results shows that the amplitude deviation of the occurred fault frequencies are very small. Picot et al. [8] and Obeid et al. [9] propose a method for the detection based on the statistical analysis of the stator current harmonics of a PMSM. The fault index bases on the frequencies multiple of the rotation frequency within the stator current spectrum. The measurements are done at specified constant speeds under no load condition. The damaged bearing can be recognized with the proposed approach, but the damage can not be differentiated from other damages causing a change in the frequencies multiple of the rotation frequency. Silva [10] presents a detection method of bearing damage based on the stator current of an induction machine similar as in [11], [12], [13]. However, the stator current is analyzed by means of the Extended Park's Vector. The considered bearing damages are holes in the outer race with three different sizes. The damage can be recognized especially for the damage with the wide diameter.

Summary, the majority of the papers study artificial wide damage and the machine is loaded with the load torque only. The influence of the radial force is not considered. Moreover, the detection by means of the Fourier and Wavelet transform are commonly employed. However, it is still a challenging issue because the deviation observed between the healthy and the faulty bearing is very small. In this paper, the stator current signal is analyzed by means of the Fourier transform

978-1-4799-7743-7/15/$31.00

with the Welch's method. Instead of the observed deviation in the current spectrum, it considered a feature set of statistical values for the detection. The statistical values are calculated from the energy content of each characteristic fault frequency within a specific interval. Statistical features are combined using the linear discriminant analysis (LDA) for the fault diagnosis. The LDA is commonly used in order to obtain a maximum separation between the feature of each group. The new approach is evaluated at two type of damages in different load cases, in which the load torque, speed and radial force are varied.

This paper is organized as follows: a short overview of the bearing damages is given in section II, in which the used bearing for the study and its damage are presented. Section III describes the diagnosis procedure and the construction of the feature matrix. Thereby, the classification method is introduced. Section IV presents the test bench and the test procedure, while the bearing damages diagnosis by means of the proposed approach is presented in section V. Finally, the work is summarized and concluded in section VI.

II. Bearing damage

Rolling bearings consist of an inner and outer race, which are separated by rolling elements such as balls or cylindrical rollers. Due to material fatigue or wearing, pitting or flaking can occur within the bearing components. If a damage is present in the bearing, shock pulses with characteristic frequencies occur during overrun through the damaged point. These characteristic frequencies depend of the affected part of the bearing and are calculated by means of the geometry of the rolling elements and the mechanical rotational frequency f_{rm}. The characteristic frequencies of each fault type are summarized in the following [14]:

Outer race defect:

$$f_{\text{outer}} = \frac{N_{\text{ball}}}{2} \cdot f_{rm} \cdot \left(1 - \frac{D_{\text{ball}}}{D_{\text{cage}}} \cos\beta\right) \tag{1}$$

Inner race defect:

$$f_{\text{inner}} = \frac{N_{\text{ball}}}{2} \cdot f_{rm} \cdot \left(1 + \frac{D_{\text{ball}}}{D_{\text{cage}}} \cos\beta\right) \tag{2}$$

Ball defect:

$$f_{\text{ball}} = f_{rm} \cdot \frac{D_{\text{cage}}}{D_{\text{ball}}} \cdot \left(1 - \frac{D_{\text{ball}}^2}{D_{\text{cage}}^2} \cos\beta^2\right) \tag{3}$$

Cage defect:

$$f_{\text{cage}} = \frac{1}{2} \cdot f_{rm} \cdot \left(1 - \frac{D_{\text{ball}}}{D_{\text{cage}}} \cos\beta\right) \tag{4}$$

whereas N_{ball} is the number of balls or cylindrical rollers, β the contact angle of the balls, D_{ball} the ball or roller diameter and D_{cage} the cage diameter, also known as the ball or roller pitch diameter.

Bearing damage causes a radial motion between the rotor and the stator, which leads to speed fluctuations resulting as oscillations in the motor current with the characteristic frequencies. The resulting motor current can be expressed as [16]:

$$i(t) = \sum_{k=1}^{\infty} i_k \cdot \cos\left(\omega_{\text{c}_k} \cdot t + \varphi\right) \tag{5}$$

with the angular velocity ω_{c_k} and the phase angle φ. The angular velocity can be expressed as $\omega_{\text{c}_k} = \frac{2\pi \cdot f_{\text{c}_k}}{p}$, with p the pole pair number of the used machine and the frequency $f_{\text{c},k}$. This frequency consists of the electric supply frequency f_{el} and the outer race fault frequency f_{outer} in case of an outer race damage:

$$\begin{aligned} f_{\text{c}_k} &= f_{\text{el}} + k \cdot f_{\text{outer}} \\ \text{with} \quad k &= \pm 1, \pm 2, \pm 3, ... \end{aligned} \tag{6}$$

In the following study, cylindrical-roller bearings of type *N203E.TVP2* with 11 rollers and the dimension $17\,\text{mm} \times 40\,\text{mm} \times 12\,\text{mm}$ are used. We investigate one healthy and two bearings with artificial damage in the outer race.

- Faulty group 1: an artificial slot in the outer race with a width of $w_1 = 0.25\,\text{mm}$.
- Faulty group 2: the outer race was wire eroded. The wire has a diameter of $8\,\text{mm}$, which produces a damaged point in the outer race with a width of $w_2 = 2.8\,\text{mm}$.

The damage size represents respectively $0.2\ \%$ and $2.3\ \%$ of the raceway length. The characteristic fault frequency for the outer race fault is reduced to:

$$f_{\text{outer}} = 4.25 \cdot f_{\text{rm}} \tag{7}$$

considering the geometry of the bearing and the number of balls.

III. Diagnosis procedure

The procedure used for the fault diagnosis is illustrated in Fig. 1. The spectral density of the measured stator current is estimated using the Welch's method at first. Then, the energy density is extracted for each characteristic fault frequency f_{c_k} (6) within a specific interval. The interval limits (8) depend on the frequency resolution of the Welch's method and the specified speed:

$$\begin{aligned} &[f_{\text{c}_k} - B_{\text{w}}/2 - \delta, f_{\text{c}_k} + B_{\text{w}}/2] \\ &\text{with } n = \pm 1, \pm 2, \pm 3, ... \end{aligned} \tag{8}$$

B_{w} represents the minimum distance between two fault frequencies and δ the minimum distance between the estimated

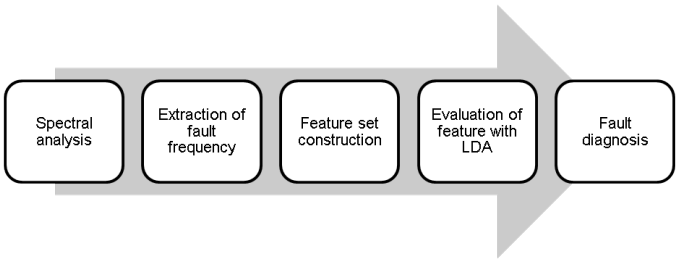

Fig. 1. Diagnosis procedure.

stator current frequencies. After the extraction, the feature matrix is constructed and evaluated by means of the LDA for the fault diagnosis. These are discussed in the following.

A. Construction of the feature matrix

The feature matrix consists of 6 statistical values calculated from each extracted frequency band. The selection of the statistical feature considering the feature, which provides good results by the fault analysis using the vibration signals [5]. These are the standard deviation, kurtosis, skewness, crest factor, clearance, shape factor and are summarized in the following:

Standard deviation:

$$x_{\mathrm{std},k} = \sqrt{\frac{1}{l}\sum_{i=1}^{l}(y_k(i) - \bar{y}_k)^2} \tag{9}$$

Kurtosis:

$$x_{kr,k} = \frac{\frac{1}{l}\sum_{i=1}^{l}(y_k(i) - \bar{y}_k)^4}{x_{std,k}^4} \tag{10}$$

Skewness:

$$x_{sk,k} = \frac{\frac{1}{l}\sum_{i=1}^{l}(y_k(i) - \bar{y}_k)^3}{x_{std,k}^3} \tag{11}$$

Crest factor:

$$x_{cr,k} = \frac{\max(y_k(i))}{y_{rms,k}} \tag{12}$$

Clearance:

$$x_{cl,k} = \frac{\max(y_k(i))}{y_{smr,k}} \tag{13}$$

Shape factor:

$$x_{sh,k} = \frac{y_{rms,k}}{\frac{1}{l}\sum_{i=1}^{l}|y_k(i)|} \tag{14}$$

with

$$\bar{y}_k = \frac{1}{l}\sum_{i=1}^{l} y_k, \quad y_{smr,k} = \frac{1}{l}\sum_{i=1}^{l}\sqrt{y_k^2}$$

$$y_{rms,k} = \sqrt{\frac{1}{l}\sum_{i=1}^{l} y_k^2}$$

where $y_k = [p_s(f_i)]$ contains the energy density of the frequencies f_i within the interval $[f_{c_k} - B_w/2 - \delta, f_{c_k} + B_w/2]$. $\bar{y}_k$ represents the mean value, $y_{rms,k}$ the root mean square (rms) value and $y_{smr,k}$ the square-mean-root (smr) value.

Instead of the standard deviation, the relative deviation Δ_r of the standard deviation $x_{std,k}$ between the healthy and the faulty case is used as a feature:

$$\Delta_r(x_{std,k}) = \frac{(|x_{std,k,healthy}| - |x_{std,k,faulty}|)}{|x_{std,k,healthy}|} \quad \text{with} \quad k = \pm1, \pm2, \pm3, ... \tag{15}$$

The feature matrix $\underline{X}$ contains the statistical values for each extracted frequency interval:

$$\underline{X} = \begin{bmatrix} x_{kr,1} & x_{sk,1} & x_{cr,1} & x_{cl,1} & x_{sh,1} & \Delta_r(x_{std,1}) \\ x_{kr,2} & x_{sk,2} & x_{cr,2} & x_{cl,2} & x_{sh,2} & \Delta_r(x_{std,2}) \\ ... & ... & ... & ... & ... & ... \\ x_{kr,k} & x_{sk,k} & x_{cr,k} & x_{cl,k} & x_{sh,k} & \Delta_r(x_{std,k}) \end{bmatrix} \tag{16}$$

B. Evaluation of the feature matrix by means of the LDA

The discriminant analysis consists of a linear combination of the feature in order to reduce the feature space and scale the feature according to its importance. Hence, a good separation between the feature set in each group can be achieved. The discriminant function calculates a discriminant value $C_i(g)$ for each observation i of the group g with the feature value x_{ij} as follows [15]:

$$\begin{aligned} C_i(g) &= b_0 + b_1 \cdot x_{i1} + b_2 \cdot x_{i2} + ... + b_j \cdot x_{ij} \text{ with} \\ x_{ij} &= \text{feature value } ij \quad (j = 1, ...6) \text{ and } (i = 1, ...n) \\ b_j &= \text{discriminant coefficient for the feature } j \\ b_0 &= \text{constant value} \end{aligned} \tag{17}$$

The discriminant coefficients are determined by maximizing the discriminant criteria Γ,

$$\Gamma = \frac{S_b}{S_w} \tag{18}$$

which is the proportion between the between-group scatter matrix S_b and the within-group scatter matrix S_w. This optimization problem can be solved as a classical eigenvalue problem. The between-group scatter matrix evaluates the separability of different groups, while the within-class scatter matrix evaluates

the compactness within each group and the between-group scatter matrix. These are defined as:

$$S_{\mathrm{b}} = \sum_{g=1}^{G} l_g(\mu_g - \mu)(\mu_g - \mu)^T \tag{19}$$

$$S_{\mathrm{w}} = \sum_{g=1}^{G} \sum_{i=1}^{l_g} (x_i(g) - \mu_g)(x_i(g) - \mu_g)^T \tag{20}$$

$$\text{with } \mu_g = \frac{1}{l_g} \sum_{i=1}^{l_g} x_i(g) \text{ and } \mu = \frac{1}{l} \sum_{i=1}^{l} x_i$$

For the fault diagnosis, the Bayes classifier is used to assign the discriminant values to each group. This is given by the posterior probability that a parameter Y_i belongs to the group g:

$$\begin{aligned} P(g|Y_i) &= \frac{P(Y_i|g)P(g)}{\sum_{g=1}^{G} P(Y_i|g)P(g)} \qquad (g = 1, 2, ..., G) \\ &= \frac{\exp\left(-\frac{D_{ig}^2}{2}\right)P(g)}{\sum_{g=1}^{G} \exp\left(-\frac{D_{ig}^2}{2}\right)P(g)} \end{aligned} \tag{21}$$

where $P(g)$ is the prior probability of the group g and D_{ig} represent the distance between the parameter Y_i and the centroid of the group $\overline{C}(g)$. This is defined as the mean value of the discriminant value for each group g: $\overline{C}(g) = \frac{1}{k} \sum_{i=1}^{k} C_i(g)$. The parameters are assigned to the group with the maximum posterior probability.

IV. Test Procedure

The test bench used for the experiments consists of a vector-controlled PMSM, a magnetic brake (load) and a cylindrical-roller bearing in a special test-bench housing. The data of the used machine are given in Appendix A. Fig. 2 shows the schematic setup of the test bench. A further description is given by [17]. The bearing housing is connected to the machine and the load through shaft couplings and is equipped with accelerometers to measure the vibration in addition. Due to the fact that a small radial load acts on the bearing of an electrical motor because of the load torque, an additional radial force is considered in this paper in order to study its influence on the bearing damage detection. Furthermore, the test motor is a drum-integrated motor for a band-conveyor, which operates permanently under radial load condition. In order to apply an adjustable radial force to the bearing, a load mechanism is included in the housing of the bearing. The force is measured by a force transducer and the bearing outer race is positioned in such a way that the applied force acts exactly on the damaged area. The currents measured within the power source are used for the machine control and for the bearing fault diagnosis. The sampling frequency for the current measurement is 100 kHz and the measured current is filtered by a second-order Butterworth filter with a cut-off frequency of 12.5 kHz.

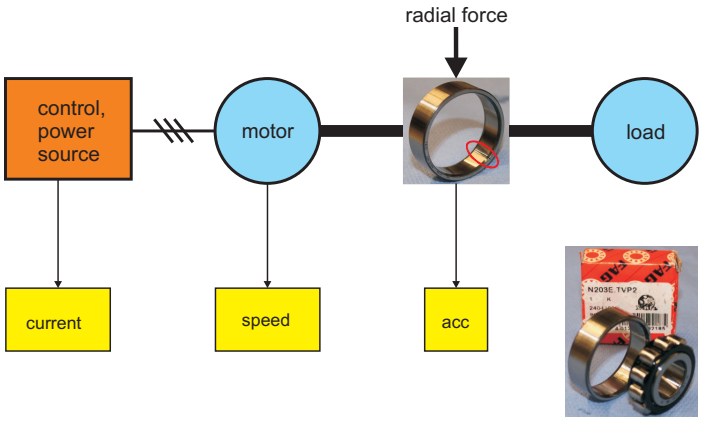

Fig. 2. Schematic setup of the test bench.

V. Bearing Damage Diagnosis

The proposed approach is evaluated by means of the measured stator current. The current signals are collected for the healthy and the damaged bearings under different operating points. The damaged bearings are with outer race fault with two different severity levels, which are presented in section II. Two phases of the stator current are measured: i_{u} and i_{v}. The motor is driven at different speeds, load torques and radial forces. The values of the speed are 400 rpm, 900 rpm and 1500 rpm. The load torque is constant at 0.1 Nm, while the radial force is set to 400 N, 1 kN or 2 kN. For the investigation, measurements are performed in the following operation points.

1) LC1: $F = 1\,\mathrm{kN}, T = 0.1\,\mathrm{Nm}, s = 900\,\mathrm{rpm}$,
2) LC2: $F = 2\,\mathrm{kN}, T = 0.1\,\mathrm{Nm}, s = 400\,\mathrm{rpm}$,
3) LC3: $F = 2\,\mathrm{kN}, T = 0.1\,\mathrm{Nm}, s = 1500\,\mathrm{rpm}$,
4) LC4: $F = 400\,\mathrm{N}, T = 0.1\,\mathrm{Nm}, s = 1500\,\mathrm{rpm}$,
5) LC5: $F = 400\,\mathrm{N}, T = 0.1\,\mathrm{Nm}, s = 400\,\mathrm{rpm}$.

The power spectral density (PSD) of the stator current is estimated for each measurement at first. Then, only the first 20 characteristic frequency bands are extracted from each stator current spectrum, because these are the most significant ones as shown in the previous paper [18]. These extracted frequency bands are finally reduced to 11 bands according to the following criteria:

- Every frequency multiple of the electrical supply frequency and the specified speed is eliminated
- Every frequency inside a frequency interval with boundaries, which includes the multiple of the electrical supply frequency is eliminated.

The eliminated frequencies can occur in the stator current spectrum with a larger amplitude than the one at the fault frequencies, so that the diagnosis results can be falsified. The PSDs of the stator current i_{u} are illustrated as an example in Fig. 3, in which two of the extracted frequency bands are

marked. This current are measured in the healthy and the faulty group 2 by the load case LC3. After the extraction, the statistical features from (10) to (14) are calculated for the extracted frequency bands for each phase current in each group and load case. Hence, a specific group contains an 22-by-6 feature matrix (16) for each load case.

The contribution of each feature in the fault detection is evaluated for all the considered load cases. This represents the percentage of the mean value for each feature vector. The results are summarized in Table I for the faulty group 1. Thereby, all values greater than 25% are represented with +; values smaller than 10% are represented with - and the middle values are represented with o. The contribution of the feature for the faulty group 2 is similar to the faulty group 1. The most significant feature in the considered load conditions is the crest factor. The skewness and the shape factor are least important, while all the other features contribute differently depending on the load condition. A fault detection by means of a single feature is not sufficient. Fig. 4 illustrates the relative deviation of x_{std} for the 11 extracted frequency intervals in the phase current i_{u} for all considered groups and three load cases. A considerable deviation is observed at some frequencies particularly in the faulty group 2. However, the deviations at the load cases $F = 1\,\mathrm{kN}, M = 0.1\,\mathrm{Nm}$ and $speed = 900\,\mathrm{rpm}$ are very small.

Therefore, the fault detection is investigated by means of the linear discriminant analysis, in which a linear combination of all features, named discriminant function, is used for the detection. The used discriminant coefficients are pre-calculated by means of a training set, which consists of the observations obtained from the measurements with the most significant characteristic harmonics. This measurement corresponds to the load case (LC2) with a total of 20% of the generated data in each group. The remaining data of all the other load cases are used as test data. The discriminant function of the training data for all groups are illustrated in Fig. 5. The line represents the separator between the healthy and the faulty state. Only 2 values of the healthy state and the faulty group 2 are false assigned, while 8 values of the faulty group 1 are false assigned. However, most values of the faulty bearing are located above the line. Hence, the faulty states can be clearly distinguished from the healthy ones by the training data.

TABLE I. CONTRIBUTION OF THE FEATURE IN THE FAULTY GROUP 1 AND IN EACH LOAD CASES.

Loadcase	x_{cr}	x_{cl}	x_{kr}	x_{sh}	x_{sk}	$\Delta_r(x_{std})$
LC1	+	o	o	-	-	-
LC2	o	o	-	-	-	+
LC3	+	o	o	-	-	-
LC4	+	o	o	-	-	-
LC5	+	o	o	-	-	o

The fault diagnosis is performed for all measured data using the Bayes classifier (21) and the results are summarized in Table II, in which the posterior probability of the affiliation to each group is represented. For the bearing damage with $0.2\,\%$ damage size (faulty group 1), $64\,\%$ of the values are assigned to the faulty state at the radial load $F = 1\,\mathrm{kN}$ and the specified speed $900\,\mathrm{rpm}$ (LC2), while $36\,\%$ are assigned to the healthy state. The other measurements provide better results from $73\,\%$ to $82\,\%$ except in the load case (LC5), in which $64\,\%$ of the values are incorrectly assigned. The bearing damage can not be distinguished in the small load condition. The same behavior is observed in the bearing damage with $2.8\,\%$ damage size (faulty group 2). The measurements with

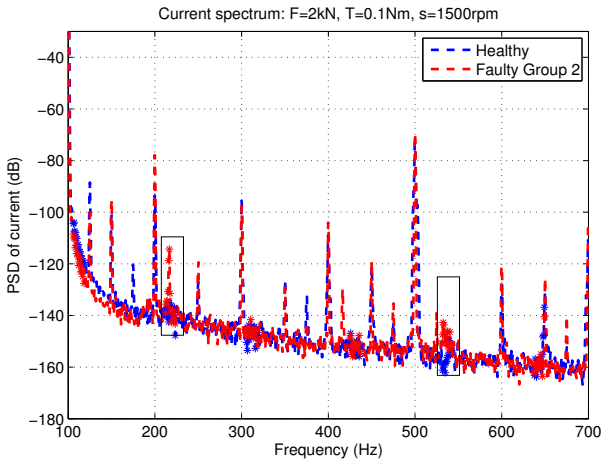

Fig. 3. Current spectrum of the healthy bearing and the faulty bearing (faulty group 2).

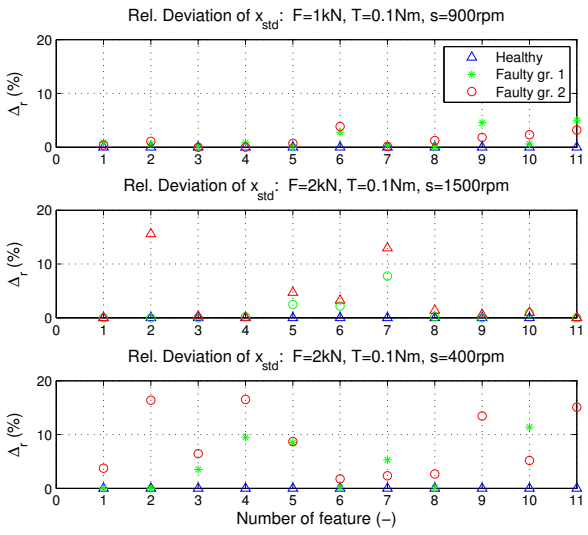

Fig. 4. Relative deviation of x_{std} for three load cases (LC1, LC2, LC3) and all groups.

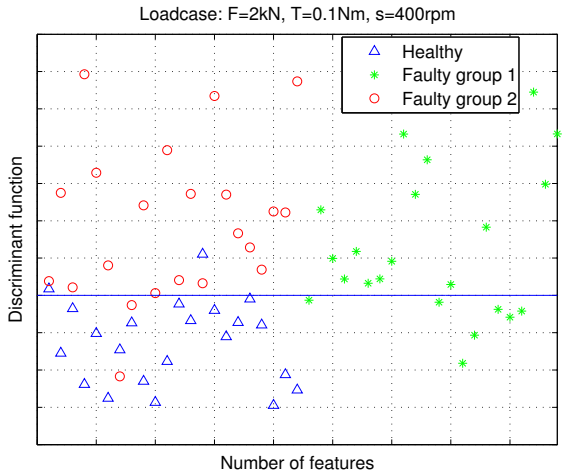

Fig. 5. Discriminant function of the training data, faulty group 1 and faulty group 2 in comparison to the healthy state at radial force 2 kN and speed $speed = 400\,\mathrm{rpm}$.

higher radial forces or speeds show better results, especially at the load case LC2, in which the posterior probability is 91 %. Any bearing damage causes a radial motion between the rotor and the stator, which leads to a rise of the friction torque in load case. The amplitude of the characteristic frequency increases with the amplitude of the friction torque which depends on the speed and the radial load. At small radial loads and speeds, the characteristic frequencies appear with an amplitude close to the noise amplitude. Hence, a fault diagnosis is impossible at this condition. Overall, the bearing damages can be distinguished by means of the proposed approach considering the applied load cases with the exception of the small load case.

VI. Summary and Conclusions

This paper presents a new approach for the diagnosis of the bearing damage by means of the stator current signal of the PMSM. The method uses the energy content in the characteristic fault frequency in order to generate specific features for the detection. These statistical features are summarized in a feature matrix and evaluated using the LDA. For the evaluation, two bearing damages are investigated and the stator current is measured for different load cases. Thereby, the fault diagnosis is performed by means of the Bayes classifier. The bearing damage can be identified and distinguished from the healthy bearing with the proposed method by the considered load cases except in the load conditions with small speeds and radial forces. Hence, the fault diagnosis is impossible in small load conditions. However, this method provides promising results for the detection of the bearing damage using the stator current and it should be evaluated for other damages such as inner race, ball or cage damages.

Appendix A

TABLE III. Data of the test motor (rated values).

	PMSM
power	500 W
pole pair	4
current	2.3 A
speed	$3000\,\mathrm{min}^{-1}$
torque	1.6 Nm
moment of inertia	$0.4239\,\mathrm{kgcm}^2$
direct inductance L_{sd}	28.6 mH
quadrature inductance L_{sq}	31.6 mH
resistance R_s at $20°C$	5.6 Ω

References

[1] P. Tavner, L. Ran, J. Penman and H. Sedding: “Condition monitoring of rotating electrical machines”, IET Power and Energy Series, 56, 2008.

[2] P. O’Donnell, IEEE Motor Reliability Working Group. “Report of large motor reliability survey of industrial and commercial installations, part I”, IEEE Transactions on Industry Applications, vol. IA-21, no. 4, pp. 853-864, July 1985.

[3] Zhou, W.; Lu, B.; Habetler, T. and Harley, R.: “Incipient Bearing Fault Detection via Motor Stator Current Noise Cancellation Using Wiener Filter”, IEEE Transactions on Industry Applications, 2009, vol.45, pp. 1309 - 1317.

[4] Delgado, M.; Cirrincione, G.; Garcia, A.; Ortega, J. A. and Henao, H.: “A novel condition monitoring scheme for bearing faults based on Curvilinear Component Analysis and hierarchical neural networks”, XXth International Conference on Electrical Machines, ICEM 2012, pp. 2472,2478, 2-5 September 2012.

[5] Jin, X.;Zhao,M.; Chow, T. W. S.; and Pecht, M.: “Motor bearing fault diagnosis using trace ratio linear discriminant analysis”, IEEE Transactions on Industrial Electronics, vol. 61 (5), pp. 2441 - 2451, 2014.

[6] Schoen, R.R.; Habetler, T.G.; Kamran, F.; Bartfield, R.G.: “Motor bearing damage detection using stator current monitoring”, IEEE Transactions on Industry Applications, vol. 31, no. 6, pp. 1274 - 1279, November - December 1995.

[7] Rosero, J.; Romeral, L.; Rosero, E. and Urresty, J.: “Fault Detection in dynamic conditions by means of Discrete Wavelet Decomposition for PMSM running under Bearing Damage”, Twenty-Fourth Annual IEEE Applied Power Electronics Conference and Exposition, APEC 2009, pp. 951 - 956, 15-19 February 2009.

[8] Picot, A.; Obeid, Z.; Regnier, J.; Maussion, P.; Poignant, S.; Darnis, O.: “Bearing fault detection in synchronous machine based on the statistical analysis of stator current”, IECON 2012 - 38th Annual Conference on IEEE Industrial Electronics Society, pp. 3862 - 3867, 25-28 October 2012.

[9] Z. Obeid, S. Poignant, J. Regnier, P. Maussion. “Stator current based indicators for bearing fault detection in synchronous machine by statistical frequency selection”, IECON 2011 - 37th Annual Conference on IEEE Industrial Electronics Society, pp. 2036-2041, 2011.

[10] Silva, J. and Cardoso, A. J. M.: “Bearing failures diagnosis in three-phase induction motors by extended Park’s vector approach”, 31st Annual Conference of IEEE Industrial Electronics Society, IECON 2005, vol. 6, pp. 2591 - 2596, 6-10 November 2005.

[11] Obaid, R. R.; Habetler, T. G. and Stack, J. R.: “Stator current analysis for bearing damage detection in induction motors”, 4th IEEE International Symposium on Diagnostics for Electric Machines, Power Electronics and Drives, SDEMPED 2003, pp. 182 - 187, 2003.

TABLE II. POSTERIOR PROBABILITY OF THE AFFILIATION TO EACH GROUP.

	Faulty group 1					**Faulty group 2**				
	LC1	LC2	LC3	LC4	LC5	LC1	LC2	LC3	LC4	LC5
Healthy	18 %	36 %	23 %	27 %	64 %	32 %	9 %	18 %	45 %	64 %
Faulty	82 %	64 %	77 %	73 %	36 %	68 %	91 %	82 %	55 %	36 %

[12] Immovilli, F.; Cocconcelli, M.; Bellini, A. and Rubini, R.: "Detection of Generalized-Roughness Bearing Fault by Spectral-Kurtosis Energy of Vibration or Current Signals", IEEE Transactions on Industrial Electronics, vol. 56, pp. 4710 - 4717, 2009.

[13] Soualhi, A.; Clerc, G.; Razik, H. and Lebaroud, A.: "Fault detection and diagnosis of induction motors based on hidden Markov model", XXth International Conference on Electrical Machines, ICEM 2012, pp. 1693 - 1699,0-5 September 2012.

[14] J. Stack, T. Habetler and R. Harley, "Fault classification and fault signature production for rolling element bearings in electric machines," 4th IEEE International Symposium on Diagnostics for Electric Machines, Power Electronics and Drives, SDEMPED 2003, pp. 172 - 176, 24-26 August 2003.

[15] S. Mika, G. Ratsch, J. Weston, B. Scholkopf, K. Muller: "Fisher discriminant analysis with kernels," Proceedings of the 1999 IEEE Signal Processing Society Workshop Neural Networks for Signal Processing IX, pp. 41 - 48, 1999.

[16] M. Blödt, P. Granjon, B. Raison and G. Rostaing, "Models for Bearing Damage Detection in Induction Motors Using Stator Current Monitoring, " IEEE Trans. on Industrial Electronics, vol. 55, no. 4, pp. 1813 - 1822, April 2008.

[17] Lessmeier,C.; Piantsop Mbo'o,C.; Coenen,I.; Zimmer, D. and Hameyer, K.: "Untersuchung von Bauteilschäden elektrischer Antriebsstränge im Belastungsprüfstand mittels Statorstromanalyse", ANT Journal, Technische Fachzeitschriften der Vereinigten Fachverlage GmbH, vol. 1, pp. 8 - 13, 2012.

[18] Piantsop Mbo'o,C.; Herold, T. and Hameyer, K.: "Impact of the load in the detection of bearing faults by using the stator current in PMSMs", XXI IEEE International Conference on Electrical Machines, ICEM 2014, pp. 1615 - 1621, 2014.

APPENDIX B

Christelle Piantsop Mbo'o was born in 1982 in Douala, Cameroon. She received her Dipl.-Ing. degree in electrical engineering in 2008 from RWTH Aachen University, Germany. Since 2009 she has been a researcher at the Institute of Electrical Machines (IEM). Her research interests include analysis and design of electrical machines.

Dr. Kay Hameyer (FIET, SMIEEE) received his M.Sc. degree in electrical engineering from the University of Hannover and his Ph.D. degree from the Berlin University of Technology, Germany. After his university studies he worked with the Robert Bosch GmbH in Stuttgart, Germany as a Design Engineer for permanent magnet servo motors and vehicle board net components. Until 2004 Dr. Hameyer was a full Professor for Numerical Field Computations and Electrical Machines with the KU Leuven in Belgium. Since 2004, he is full professor and the director of the Institute of Electrical Machines (IEM) at RWTH Aachen University in Germany. 2006 he was vice dean of the faculty and from 2007 to 2009 he was the dean of the faculty of Electrical Engineering and Information Technology of RWTH Aachen University. His research interests are numerical field computation and optimisation, the design and controls of electrical machines, in particular permanent magnet excited machines, induction machines and the design employing the methodology of virtual reality. Since several years Dr. Hameyer's work is concerned with the development of magnetic levitation for drive systems, magnetically excited audible noise in electrical machines and the characterisation of ferro-magnetic materials. Dr. Hameyer is author of more then 250 journal publications, more then 500 international conference publications and author of 4 books. Dr. Hameyer is a member of VDE, IEEE senior member, fellow of the IET.